

Conceptual design and optimization of the LEAF hybrid aircraft: a step towards the future.

Vincenzo Mazzone, Andrea Fiorino, Francesco Antonio Marrocco, Vincenzo Donato

^aDepartment of Engineering for Innovation, Università del Salento, Campus Ecotekne, Italy

Abstract

In latest years, environmental policies have been conducted for the aviation sector to obtain less polluting propulsion. All-electric aircraft offer the possibility to eliminate direct fuel combustion emissions, but their development is blocked by battery energy limits and power density. Therefore, hybrid propulsion systems have emerged as a potential solution, as they have demonstrated a good compromise between performance and low polluting emissions. This work proposes an alternative solution to the powertrain of a regional aircraft by testing a hybrid configuration created with the aid of technologies that can be developed by 2040. Using the ATR 42 aircraft as a reference, the propulsion system was equipped with two turboprop and four electric motors, powered by both batteries and supercapacitors, the latter used in the take-off phase due to the high power density, they also have a structural function thus allowing a reduction in weight. The Wing-Load is estimated by the most critical condition that is the take-off phase through the take-off parameter to respect the required field length; the needed engine power is calculated for each flight phase. Finally, an analysis of the fuel consumption during the mission, of the emissions produced based on the origin of the energy sources, a survey on the costs, safety and environmental impact due to the disposal of the storage systems are reported to verify the sustainability of the solution.

Keywords: Regional Aircraft, Hybrid electric propulsion system, Sizing, NSGA,



1. Introduction

The CO_2 and NO_x are the most relevant problem in 2022 for the conventional aircraft. Before the COVID-19 pandemic (2019) the airline industries spent for the fossil fuel \$ 188 billions, The COVID-19 pandemic has offered a chance to measure air transport's impact on the environment, the pause in travel resulted in an 8 percent drop in CO_2 emissions in 2020 [1]. During this situation the research has moved to control the emissions due to carbon dioxide, some researches has moved into the hydrogen cells, others in the control of the emissions at ground; actually the most reasonable choice is the renewable energy that is the electric energy. Flying produces on average 285 grams of carbon dioxide per passenger for each kilometer traveled, for a 800 km regional fly and 50 passengers the estimate is: 11.5 ton of carbon dioxide. According to Friedrich and Robertson [2], the large-scale hybridization of aircraft in the future may allow fuel savings of up to 10% compared to conventional turbofan engines but, when combined with aerodynamics, materials and structural advances, hybrid-electric propulsion reveals a potential fuel saving of 70%, together with significant benefits in terms of emissions and noise reduction. However, on the topic of hybridization the literature focuses almost exclusively on small aircraft. For these types, Köhler and Jeschke [3] compared three possible propulsion systems, namely the internal combustion engine, the parallel hybrid and the fully electric propulsion system. The results show that, for

specific power requirements, the parallel hybrid propulsion system can offer advantages in terms of system mass and cruising efficiency over the conventional internal combustion engine system. Szirczak et al. [4] instead realized a conceptual design of a small Aircraft with a hybrid propulsion system demonstrating that a low level of hybridisation results in little mass increase, baseline range and reduced energy use, but only achievable at the expense of reduced speed. Ribeiro et al. [5] justify this dominance of fossil fuel aviation for large-scale aircraft with the fact that hybrid aircraft have technical limitations in terms of operational range and seats available. Although the electrification of aircraft offers significant advantages both in terms of emissions and energy efficiency [6], with current technologies the batteries have an energy density that is not suitable for supporting large aircraft without causing an excessive increase in mass [7]. The Low Emission Aircraft of the Future (L.E.A.F.) project is born as part of the competition proposed by the Futprint50 initiative to reduce the pollution due to CO_2 through the aircraft hybridization. The design is conceptual, other phases require a lot of resources and a very large budget; this is an academic competition, so the budget and resources are very limited. The calculations are raw but provide a model that refined in the other phases of the design process. The main idea is the growth of technology, the L.E.A.F. project's takes into account the development process of the propulsion and structural components and this is designed to 2040 as foreseen by the competition. The goal of this project is a hybrid electric regional aircraft that release in the atmosphere less CO_2 than the other similar regional conventional aircraft (ATR-42 and ATR-72). The mission requirements are listed below:

- 50 passengers (5300 kg).
- Range 800 km.
- Cruise speed 0.48 Ma.
- Payload 5800 kg.
- Minimum RoC 1850 ft/min.
- Minimum FL 170 time to climb 13 min.
- Maximum operating altitude 7620 m (25000 ft).
- Minimum take-off field length 1000 m.
- Minimum landing field length 1000 m.

For the range requirement the mission is divided by submissions that are:

- Taxing.
- Take off.
- Climb.
- Cruise.
- Descent.
- Loiter.
- Climb.
- Cruise for the reserve fuel policy.
- Loiter for the reserve fuel policy.
- Landing.
- Taxing.

The paper is organized as follows. Chapter 2 describes the methodologies used to design the aircraft; in particular, Paragraph 2.1 shows how the take-off weight was estimated, Paragraph 2.2 analyzes the wing loading, Paragraph 2.3 describes how the powers requests during the flight were determined and Paragraph 2.4 studies the aerodynamics of the aircraft, reporting the dimensions of each element. We then move on to an analysis of the powertrain with paragraph 2.5 which shows the architecture considered for the aircraft and paragraph 2.6 which goes into detail on the sizing of the various components. Then, we arrive at paragraph 2.7 which describes the optimization of the applied energy management. The chapter ends with paragraph 2.8 which explains how the center of mass was estimated. Chapter 3 instead examines and discusses the results deriving from the design with an analysis on emissions in paragraph 3.1 with a comparison with respect to the reference aircraft, a cost analysis in paragraph 3.2 and a safety analysis in paragraph 3.3.

2. Methodology

2.1. Take off weight estimation

To estimate take-off weight it is necessary to calculate the empty weight, the fuel quantity and the weight fractions for each phase of the flight. For the L.E.A.F. project's the aircraft is built by the conventional materials and the the wing is fixed and it has not a sweep angle, the estimate from this consideration was made by the following formula:

$$\frac{W_e}{W_0} = A \cdot W_0^c k_c k_{vs} \quad (1)$$

Where A and c are estimated by the historical data, k_c and k_{vs} are the coefficients for the adoption to the composite materials and sweep variable geometry and W_0 is the take-off weight that is unknown. The take-off weight formula's is:

$$W_0 = \frac{W_{crew} + W_{payload}}{1 - \frac{W_f}{W_0} - \frac{W_e}{W_0}} \quad (2)$$

Replacing 1 in 2 and using the Breguet's formula for W_f is possible to estimate the take-off weight. An iterative method is used to solve the equation 2, guess initial value W_0 , after a few iterations, a value of take-off weight was obtained for an entirely thermal propulsion aircraft. Another iterative scheme was used to estimate W_{bat} , that is the weight of batteries due to the hybridization of aircraft. The electric optimal strategy is explained in the Section 1 which provides the use of electric motors in the phases of take-off and climbs while during the cruise the batteries are charged. Having an initial value W_0 , through the procedure described in Chapter 2.6.3 is possible to calculate the initial weight of batteries W_{bat} . Adding W_{bat} in the 2, after a few iterations between the adapted Breguet's formula and the modified 2, a value of take-off weight for the hybrid aircraft was obtained.

The L.E.A.F. results are:

- Maximum take-off mass: $W_0 = 42620 \text{ lb}$
- Operating mass empty: $W_e = 24012 \text{ lb}$

2.2. Wing-Loading

The crucial phase of flight is the take-off, to satisfy the requirement of the take-off field length it is necessary to choose properly the Wing-Loading.

For each phase of flight the wing loading was calculated, between all flight phases the take-off phase required the lowest wing loading. In accordance with the mission requirements it was necessary to calculate properly the wing loading, to choice properly the wing loading for the take-off phase that respect the requirement of take-off field length it was used the Take Off Parameter (TOP), this parameter is defined for each take-off field length.

The wing loading due to this approach is $62 \text{ lb}/\text{ft}^2$ that is very close an ATR vehicle.

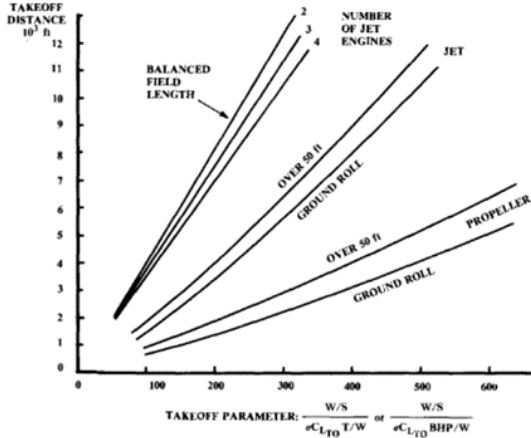


Figure 1: TOP with field length [8]

Table 1: Aerodynamics parameters of the L.E.A.F. aircraft.

Parameter	Unit	Value
Sweep Angle	deg	0
Dihedral Angle	deg	0
Taper Ratio	-	0.45
Aspect Ratio	-	9.2
S_{wet}/S_{ref}	-	5.5
E_{max}	-	14

2.3. Power requirement of flight

Each phases of flight require a power level, to estimate the weight of batteries, so the take-off weight, it is necessary to calculate the power requirement for each phase of flight. This aspect is fundamental to sizing the thermal propulsion and the electric propulsion, is obviously that is a compromise between the two powers. To calculate the power requirement of flight it was used the typical formula for a turboprop aircraft the results is shown in Figure 11. The better choice for the mission was the use of the thermal propulsion (turboprop) during the cruise, so the thermal propulsion is under-sizing respect the take-off and climbing phases and the gap of power of this phases is compensated from the electric power (electric motors). From these assumption, the electric power was calculated and the weight of batteries was sizing properly.

2.4. Aerodynamics Configuration

For a regional aircraft the velocity is so far to transonic region, so the configuration is very simply respect to the conventional civil aircraft that have a turbofan propulsion. From these consideration the L.E.A.F. aircraft have a high wing for the lateral direction stability with zero dihedral angle and zero sweep angle with a non zero taper ratio to reduce the induced drag. The dimensions of the wings are shown in Table 2 while those of the tail and those of the fuselage are shown in Table 3 and Table 4 respectively.



Figure 2: Polar aerodynamic diagram referred to the cruise phase.

Table 2: Wing Size of the L.E.A.F. aircraft.

Parameter	Unit	Value
Span	ft	82
S_{ref}	ft ²	718
S_{wet}	ft ²	3950
C_{root}	ft	12.2
C_{tip}	ft	5.5
MAC	ft	9.26

Table 3: Tail Size of the L.E.A.F. aircraft.

Parameter	Unit	Value
b_{ht}	ft	33.8
S_{ht}	ft ²	124
b_{vt}	ft	30
S_{vt}	ft ²	66.7

Table 4: Fuselage Size of the L.E.A.F. aircraft.

Parameter	Unit	Value
Length L	ft	91.04
Diameter D	ft	11.38

The aircraft have a slotted flap that increase lift coefficient to 2.2 (C_{lmax}), therefore from some considerations is possible to estimate the lift coefficient for take-off or landing and the drag coefficient.

It was possible to estimate the polar aerodynamics using an academic software, the Figure 2 shown the results in cruise at different velocity.

2.5. Powertrain Configuration

Figure 3 presents a scheme of the aircraft architecture that it has been decided to use. As regards the arrangement of the propellers, the solution proposed by Hoelzen et al. [10] was used, the latter is characterized by two turboprop side by side parallel to four electric motors, this choice was determined by a much higher reliability of the electric motors compared to the engines,

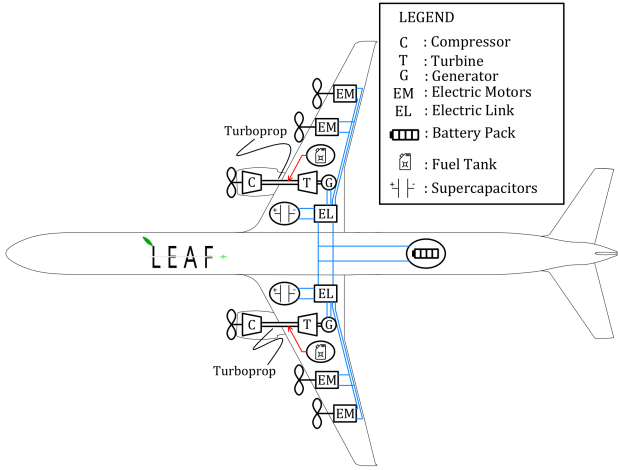


Figure 3: Aircraft architecture. (Aircraft silhouette taken by [9])

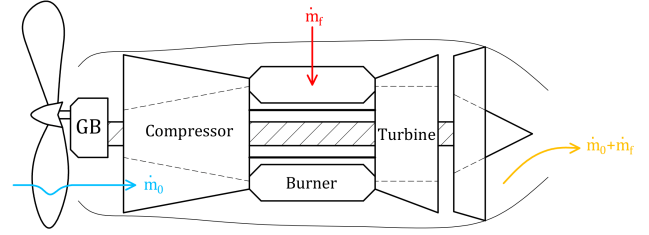


Figure 4: Schematic drawing of a turboprop engine. [18]

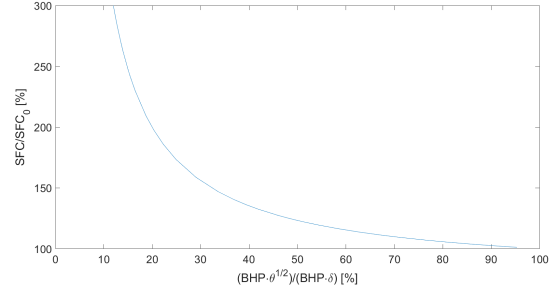


Figure 5: Performance Curve of a Turboprop Engine.

for this reason a greater number of them were used. Each electric motor then needs an inverter that converts the DC voltage into AC voltage [11], these are components with high efficiency [12], their efficiency has therefore been assumed to be consistently 98%. Although the contribution of electric motors brings a significant advantage in terms of sustainability and reliability, the electrical energy storage systems suffer from a very low energy density which leads to low use [13]. In addition to this, it is known that batteries exhibit degradation phenomena due to various factors, including time and use [14]. To overcome this problem, for the power supply of the electric motors it was decided to add supercapacitors to the batteries, which, despite the even lower energy density and extremely short discharge times, are characterized by a high power density as well as the absence of degradation phenomena because they are purely electrical rather than electrochemical devices [15]. By virtue of the listed characteristics, supercapacitors are used in phases in which there is a high demand for power in order to limit the current outgoing from the battery pack in order to increase its Cycle Life. Furthermore, materials with both a structural function and that of supercapacitors are recently in the experimental phase [16], it was therefore chosen to take advantage of this solution in such a way as to obtain a reduction in weight. Finally, during the continuation of the mission there are phases in which the battery is recharged by the heat engines, this first of all allows the turboprop to work in conditions of greater efficiency but in addition to this a reduction of the Depth of Charge of the battery pack is allowed by increasing so the Cycle Life. The above is made possible by inserting an electricity generator downstream of the turboprop connected to the battery pack by means of an Electric Link, this solution was also adopted by Glasscock et al. [17].

2.6. Powertrain Components Analysis

2.6.1. Engines

As previously mentioned, as regards fuel-assisted propulsion, it was decided to use turboprop whose scheme is shown in Figure 4. Specific Fuel Consumption (SFC) is analyzed as

a function of the corrected power ratio $BHP/BHP_0 \cdot \sqrt{\theta}/\delta$, where θ and δ are the pressure and temperature ratios, respectively. The air pressure and temperature input values can be determined as [19]:

$$T_{inlet} = T_{amb} \cdot \left(1 + \frac{\gamma - 1}{2} \cdot Mach^2\right) \quad (3)$$

$$p_{inlet} = p_{amb} \cdot \left(1 + \frac{\gamma - 1}{2} \cdot Mach^2\right)^{\frac{\gamma - 1}{\gamma}} \quad (4)$$

The ratio between constant pressure and constant volume specific heats for air, γ , is assumed equal to 1.4. The ambient pressure and temperature values T_{amb} and p_{amb} , together with the speed of sound needed to determine the Mach number, were obtained from altitude-dependent tabulated values found in the literature [20]. To size the turboprop, it was made so that during the cruise phase, known to be the most influential phase of fuel consumption, there is a corrected power ratio equal to 1, thus ensuring that the engine has maximum efficiency. Therefore, from this reasoning we chose the PW125B engine characterized by a nominal power equal to 2500hp and a specific consumption equivalent to 0.463lb · hp⁻¹h⁻¹ [21]. Then, the specific fuel consumption is determined at each instant of time by means of an approach proposed by Fletcher and Walsh [22] in which a function of the corrected power ratio is considered with a trend shown in Figure 5. Therefore, the specific consumption related to each instant of the mission is known, multiplying the latter by the instantaneous power of the thermal engine obtains the fuel flow necessary to power the thermal part of the aircraft.

2.6.2. Electric Motors

It has been demonstrated that electrical motors provide an ideal means for achieving aircraft propulsion [23]. For the choice of the electric motor, it was ensured that in the take off

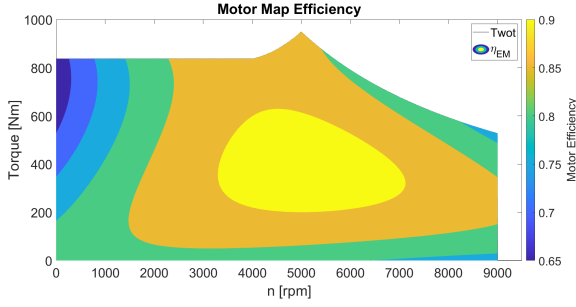


Figure 6: Electric motor efficiency map.

Table 5: Cell specifications.

Parameter	Unit	Value
Voltage	V	3.6
Capacity	Ah	10.15
C_{rate}	C	5
Weight	g	73
Volume	cm^3	26

Table 6: Specification of the battery sized in this investigation.

Parameter	Unit	Value
Mass	kg	1431
Capacity	Ah	710.5
Energy	MWh	0.50
Power	MW	2.51
Maximum Discharge Current	A	3553
Maximum Charge Current	A	710.5

phase, corresponding to the period of time in which there is the highest power request of the mission, the necessary power is guaranteed taking into account both the contribution of the electric motors and the contribution of the turboprop, for the latter it was decided to consider a power in the take off phase equal to the power required in the cruise phase. Consequently, from the literature [24] it was chosen to use a motor having the torque curve shown in Figure 6. The efficiency map was instead obtained by considering the efficiency of a generic electric motor. For electric propulsion, a propeller with a fixed number of revolutions was preferred, imposing a rotational speed of 5000 rpm, thus splitting the power required by the single electric motor for the set speed, the torque that must be delivered at all times and the resulting working point of the engine to which its efficiency corresponds is obtained. As a result, increasing the power required for the efficiency of the electric motor results in the instantaneous power to be supplied by the electricity accumulators.

2.6.3. Batteries

The main electricity storage system that is used is made up of batteries; in this period the market is dominated by lithium-ion batteries due to their high specific energy and their availability on the market [25]. Currently, the electrification of the aircraft is very challenging, with the scale of the challenge increasing with size and range [26]. The main reason for these difficulties lies in the low energy density, equal to about $250Wh/kg$, which still characterizes batteries today [27]. According to Tiede et al. [28], in the year 2040 the batteries will be characterized on average by an energy density of $500Wh/kg$. Batteries also have a power requirement, the latter being evaluated on the basis of the C_{rate} , which is defined as the maximum current of the battery for continuous discharge divided by its nominal capacity [29]. Generally, the high-power phases of missions may require a 4-5 C discharge [26]. On the basis of these data and on a comparison between the cells currently available on the market, a possible cell having the described characteristics has been hypothesized, the parameters of this cell are summarized in Table 5.

Given the sporadic use of electric motors, it was decided to use a power requirement as a primary requirement for sizing the battery pack. In particular, given that in the take off phase

the battery pack is assisted by supercapacitors, the climb phase is used to establish the maximum power that can be delivered by the batteries, ensuring that the thermal engines maintain a power constantly equal to the power required during the cruise. In addition to this, for safety reasons it was decided to add an energy requirement of $500kWh$. First of all, the number of cells to be placed in series is determined, this is chosen in such a way that the battery pack has an output voltage equal to the nominal voltage of the electric motor, the latter is equal to 700 V, then this voltage is divided for the nominal voltage obtaining the number of cells in series that make up a single string. The string of cells in series is characterized by a power equal to the product of the number of cells in series N_s by the cell voltage V_c by the nominal capacity C_{nom} of the single cell multiplied by the discharge C_{rate} :

$$P_s = N_s \cdot V_c \cdot C_{nom} \cdot C_{rate} \quad (5)$$

The same string contains an energy equal to the product of the capacitance times the cell voltage multiplied by the number of cells in series:

$$E_s = N_s \cdot V_c \cdot C_{nom} \quad (6)$$

Thus, the number of strings to be inserted in parallel is obtained considering the maximum value of strings required for energy or power.

Following appropriate reiterations due to the correction of the masses, a battery pack of 70 strings in parallel was obtained, characterized by 196 cells in series for a total of 13720 cells. The characteristics of the battery pack obtained are shown in Table 6 taking into account the fact that the mass has been corrected by a factor of 1.4 in such a way as to also include the wiring and the cooling system.

The batteries were then modeled using a quasi-static approach proposed by Guzzella and Sciarretta [30] using the equivalent

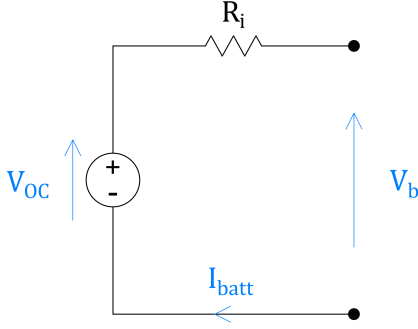


Figure 7: Equivalent circuit of the battery.

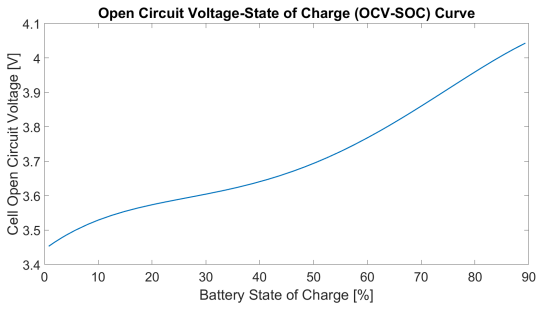


Figure 8: Trend of the open circuit voltage as the state of charge varies.

electrical circuit shown in Figure 7, the latter being characterized by an open circuit voltage V_{OC} and an internal impedance R_i . Knowing the power required at each instant, solving the circuit shown in Figure 7 we obtain the relationship:

$$P_{batt} = (V_{OC} - R_i I_{batt}) I_{batt} \quad (7)$$

Where the unknown is represented by the current I_{batt} , it is therefore necessary to solve a second degree equation at all times in order to determine the current output from the battery pack and therefore the state of charge of the cells.

As input parameters, it is known that the open circuit voltage has a non-negligible dependence on the state of charge of the battery, therefore experimental data have been obtained from the literature [31] that report the trend of the open circuit voltage as a function of the state of charge for lithium ion batteries, these data were then approximated by a polynomial function whose results are shown in Figure 8. For the internal resistance, instead, a value equal to $500m\Omega$ was considered.

It is important to point out that it is good to start with the battery not fully charged since otherwise there could be overcharging problems [32]. It was therefore decided to consider an initial state of charge equal to 90%.

As described in paragraph 2.1, a Take Off Weight is determined for the LEAF aircraft equal to:

- $W_0 = 45768 \text{ lb}$
- $W_{batt} = 3148 \text{ lb}$

2.6.4. Supercapacitors

Supercapacitors compared to batteries have significant advantages, including high power density, fast charge and dis-

Table 7: Specification of the supercapacitors considered in this investigation.

Parameter	Unit	Value
Gravimetric Capacitances	mF/g	22.24
Volumetric Capacitances	mF/cm^3	5.97
Storage Modulus	MPa	2939
Loss Modulus	MPa	632.9

charge times, low input resistance, high useful life and respect for the environment [33]. The main disadvantage of supercapacitors is the low energy density [34] as well as the fast self-discharge times [35]. For the characteristics listed, they can be combined with batteries for the electric propulsion; in fact, where the batteries have a high energy density and a low power density, supercapacitors are characterized by a high power density and a low energy density to the point of being classified as a Short Term Storage System.

It is known that the energy that can be accumulated by a capacitor is proportional to the capacity and to the square of the voltage through the relationship [36]:

$$E_{sc} = \frac{1}{2} C \cdot V_{sc}^2 \quad (8)$$

From this relationship, therefore, the necessary capacity of the supercapacitors that will be installed on the aircraft is obtained, as available energy it was decided to use the energy necessary during the entire take off phase, adding a further contribution of 20% for safety purposes. while the voltage is equal to the working voltage of the motors; that is, 700 V. Consequently, it has been obtained that the supercapacitors must have a capacity equal to $1000F$.

As far as modeling is concerned, an approach proposed by Guzzella and Amstutz [37] was used similar to that seen for the batteries; in particular, supercapacitors are modeled as an open circuit characterized by a capacitor and an internal resistance; consequently, the following relationship must be respected at all times:

$$P_{sc} = (V_{sc} - R_i I_{sc}) I_{sc} \quad (9)$$

By determining the I_{sc} current at any time, it is possible to obtain the state of charge of the supercapacitors as the ratio between the instantaneous voltage and the maximum voltage.

There are materials that have the characteristic of being multifunctional since they have the ability to perform both a supercapacitor function and a structural part thus contributing to the reinforcement of the aircraft and, therefore, obtaining a weight reduction. Javid et al. [38] have created a multifunctional material having the characteristics shown in Table 7.

It follows that for the application under analysis a supercapacitor having a mass of $45kg$ and a volume of $168l$ is required. It is necessary to specify that if the batteries had to support the take off phase it would have been necessary to add a weight of about $125kg$, so the advantages in this aspect are evident.

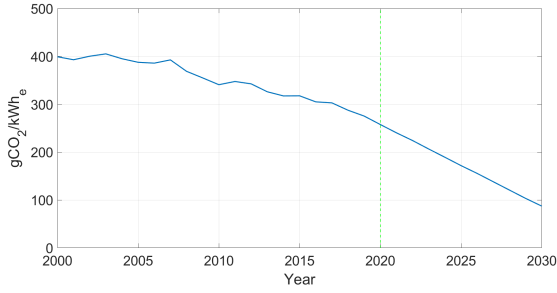


Figure 9: Trend of Greenhouse Emissions intensity vs. years (average value for EU 28 countries).

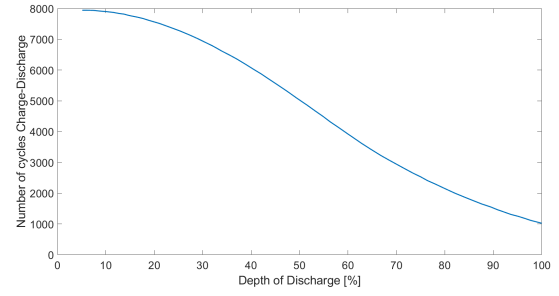


Figure 10: Dependence of the battery life on the depth of discharge.

315 2.7. Energy management optimization

2.7.1. Targets

Although polluting emissions are generally associated with heat engines, there is a contribution in this sense also from the type of source used to power the electrical counterpart [39] as well as for the production and disposal of storage systems [40]. The listed aspects are analyzed below.

As regards the emissions due to combustion, these are obtained by multiplying the mass of fuel necessary to complete the mission by the combustion factor relating to the fuel used, the latter must take into account both the combustion achieved and the contribution of the necessary logistics to transfer the fuel to the filling station:

$$CO_{2eng} = E.F. \cdot m_{fuel} \quad (10)$$

From the literature [41] it has been seen that Jet Kerosene has an emission factor of 3.25, increased to 3.8 for the reasons mentioned.

From the point of view of electric propulsion, the emissions related to the latter depend on the primary source of energy used which is not always advantageous compared to turboprop propulsion. The trend of average emissions expected up to 2030 in Europe due to the production of electricity was found in the literature [42], the result is shown in Figure 9. By extrapolating these data it can be obtained that according to these forecasts in 2040 European countries will emit on average about $75gCO_2/kWh$, multiplying this result by the necessary electricity we obtain the emissions due to the propulsion supply.

Finally, Kelly et al. [43] have analyzed the CO_2 emissions due to the production of lithium-ion batteries obtaining that the latter emits a minimum of $42kgCO_2/kWh_{batt}$, since the installed battery pack contains an amount of energy equal to $501.3kWh$, the production of the battery pack emits $21054.6kgCO_2$. To enter this value within the calculation of emissions for the single mission, it is necessary to fraction it to the Cycle Life of the batteries; that is, the number of charge and discharge cycles that the battery pack can undergo before it reaches the end of its useful life. The main parameter that influences the Cycle Life of the batteries is the Depth of Discharge (DOD), the latter represents the difference between the maximum state of charge and the minimum state of charge, therefore it defines the exploitation of the battery pack during the entire mission. Shchurov et al. [44] have analyzed this dependence obtaining

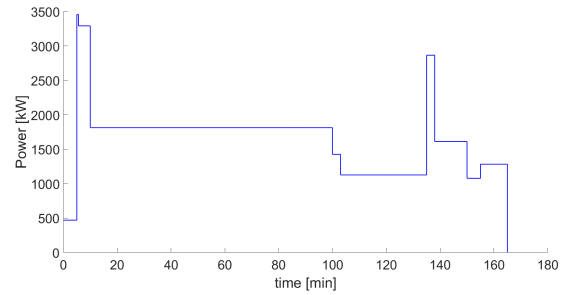


Figure 11: Total power required of the aircraft during the course of the mission.

the trend shown in Figure 10. The emissions due to disposal are not considered as they are negligible due to the fact that lithium batteries can be recycled with high efficiency [45].

Ultimately, during the mission there is an overall amount of CO_2 produced equal to:

$$CO_{2tot} = CO_{2eng} + CO_{2el} + \frac{CO_{2batt}}{Cycle\ Life} \quad (11)$$

The primary objective is the reduction of this value.

2.7.2. Description of the optimization

After making the necessary weight corrections due to the electrical energy accumulators, the trend of the total power required by the aircraft during the entire mission was obtained, the results are shown in Figure 11. With the exception of the taxing phase, in which it is preferred to use only electric propulsion in order to make airport operations cleaner and quieter [46], there are nine phases in which to define the energy management of the powertrain with the aim of minimize greenhouse gas emissions. To define energy management, a vector u is used consisting of nine components corresponding to the nine flight phases:

$$u = [u_2 \quad u_3 \quad u_4 \quad u_5 \quad u_6 \quad u_7 \quad u_8 \quad u_9 \quad u_{10}] \quad (12)$$

Each component of the vector u is defined as the ratio between the power delivered by the electric propulsion and the total power required by the aircraft:

$$u(i) = \frac{P_{el}(i)}{P_{tot}(i)} \quad (13)$$

In addition to this, it is necessary to define the contribution of the supercapacitors, to do this we consider a vector v which in

the take off phase and in the two climb phases characterizes the relationship between the power supplied by the supercapacitors and the power required by the electric accumulators in general:

$$v = [v_2 \quad v_3 \quad v_7] \quad (14)$$

$$v(i) = \frac{P_{sc}(i)}{P_{acc}(i)} \quad (15)$$

There is therefore a total of twelve variables characterizing the energy management of the aircraft. The goal is to find the optimal combination of these variables that leads to the minimization of total emissions; in addition to this, we want to preserve the useful life of the batteries by maximizing the Cycle Life [47], due to the huge costs associated with them. Finally, always with the aim of reducing costs, a minimization of fuel consumption is required.

With these premises, a multi-objective numerical optimization was used; in particular, it was decided to use the NSGA-II algorithm, this is a multi-objective optimization algorithm that is part of the genetic algorithms, the latter are a simplified version of Darwin's evolution [48]. In particular, the NSGA-II algorithm has three specific characteristics, fast non-dominated sorting approach, fast crowded distance estimation procedure and simple crowded comparison operator [49]. However, there is a real possibility that the optimization phase will lead to results without physical meaning, to overcome this, constraints are imposed such that these solutions are classified as "unfeasible", these constraints are reported below:

- The turboprop must have a corrected power ratio never higher than 1:

$$\max\left(\frac{BHP}{BHP_0} \frac{\sqrt{\theta}}{\delta}\right) \leq 1 \quad (16)$$

- The torque supplied by the single electric motor must never exceed the maximum torque that can be supplied by it:

$$\max(T_{el}) \leq T_{max} \quad (17)$$

- The battery pack current must always be between the maximum charge and discharge current limits:

$$\max(I_{batt}) \leq I_{max,dis} \quad (18)$$

$$\min(I_{batt}) \geq I_{max,ch} \quad (19)$$

- The state of charge of the battery pack must always be greater than 30% thus preserving safety and useful life:

$$\min(SOC_{batt}) \geq 30\% \quad (20)$$

- The state of charge of the supercapacitors must always be positive:

$$\min(SOC_{sc}) \geq 0 \quad (21)$$

With these premises, the optimization is performed by imposing the following objectives:

1. Overall emissions minimization.
2. Battery pack cycle life maximization.
3. Fuel consumption minimization.

We therefore started from a first generation consisting of 50 random elements and then carried out the evolution in the following 150 generations for a total of 7500 elements.

2.8. Center of gravity estimation

The position of the center of gravity of the airplane can be determined by considering the airplane system as a concentrated mass system, whereby knowing the weight of the airplane and its parts can be used to determine an estimate of the position of the center of gravity as the various components are added. The weights of the components were founded in literature, where given the empty weight of our airplane, it gives an estimate of the weight of the components. Having thus obtained these weights, by introducing a reference system with origin at the nose of the aircraft and positive direction of the longitudinal axis (X-axis) towards the nose, we have positioned the concentrated masses representing the aircraft parts and by also referring to similar aircraft configurations have estimated the position of the center of gravity. At the end of the work, the position of the center of gravity turns out to be 12.83m along the x-axis from the nose of the fuselage. However, the method used by Nicolosi et al. [50], in which the weights and relative positions of the centers of gravity of the various systems and subsystems are considered, turns out to be an approximate method, also considering that the estimate of the center of gravity was obtained assuming that the aircraft is stationary and not in flight. However, although this method is not very accurate, it was possible to obtain the position of the aircraft's center of gravity to a good approximation.

3. Results

3.1. Emissions analysis

During the simulations using the NSGA II genetic algorithm, started with the aim of determining the optimal energy management strategy for the mission, 4188 feasible solutions were derived, from these the Pareto front was extracted; in particular, a solution is called Pareto Optimal when it is not possible to improve an objective without deteriorating at least another one [51]. Figure 12 shows the solutions constituting the Pareto Front, the CO_2 emissions are shown on the abscissa axis and the Cycle Life of the battery pack on the ordinate axis. Optimization regarding fuel consumption was not considered since the most significant contribution in greenhouse gas emissions is provided by combustion, so they are directly related to fuel consumption. By comparing the solutions, it was decided to have overall emissions below $4970kgCO_2$ and a Cycle Life above 4500, thus obtaining the following solution:

$$u = [0.13 \quad 0.28 \quad 0.00 \quad 0.00 \quad 0.00 \quad 0.33 \quad 0.19 \quad 0.12 \quad 0.00] \quad (22)$$

$$v = [1.00 \quad 0.00 \quad 0.00] \quad (23)$$

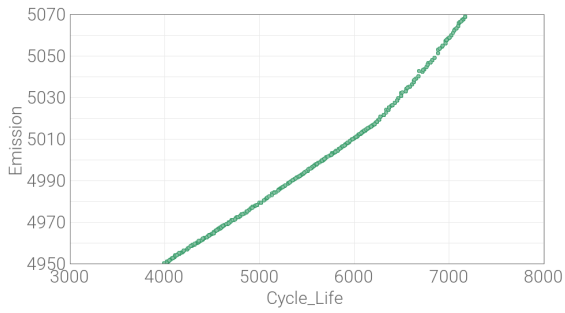


Figure 12: Pareto front of solutions concerning greenhouse gas emissions and the Cycle Life of the battery pack.

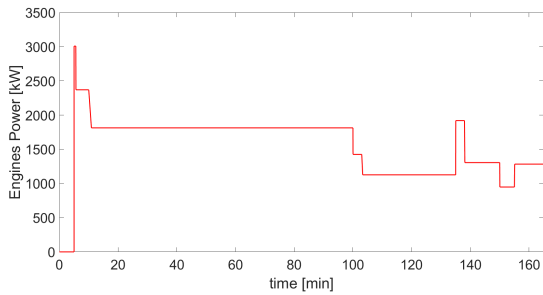


Figure 13: Trend of the overall power delivered by the turboprop during the mission.

From the optimization it was highlighted that in no flight phase is it required the recharge on board of the batteries, this allows the removal of the generators, this prerogative is appropriate because it allows to eliminate the mechanical connections between the electric machines and the turboprop, a simplification that brings also economic and mass reduction benefits.

Figure 13 and Figure 14 show the trend, following the improvement of the parameters, of the overall power delivered by the engines and electric motors respectively. It can be observed that the electric motors do not intervene in the cruise, landing and loiter phases while they support the turboprops in the high power phases, in this way it was possible to reduce the size of the turboprop. Furthermore, it should be noted that the turboprop, started in the take off phase, always remain operational, an indispensable condition to ensure that the gas in the engine follows the combustion cycle.

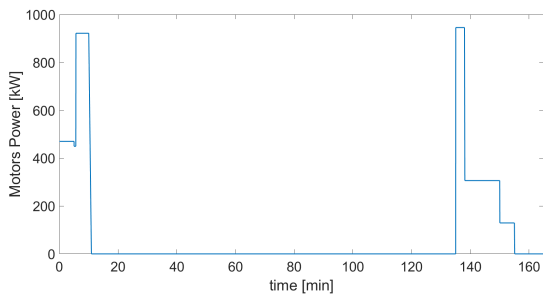


Figure 14: Trend of the overall power delivered by the electric motors during the mission.

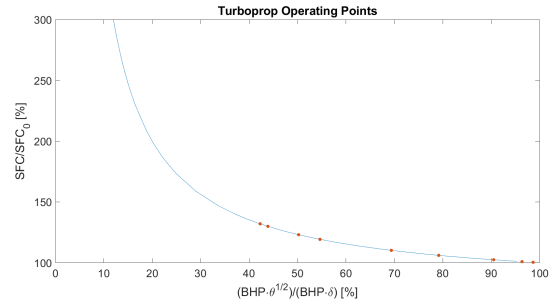


Figure 15: Operating points of the turboprop during the mission.

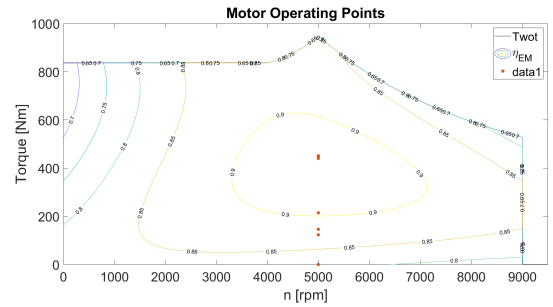


Figure 16: Operating points of the electric motors during the mission.

It is possible to analyze the influence of the powers determined on the characteristic curves of thermal and electric engines, in Figure 15 the operating points of the turboprop are shown and in Figure 16 the operating points of the electric motors on the efficiency map. Figure 17 shows the state of charge of the battery pack in the continuation of the mission while Figure 18 shows the state of charge of the supercapacitors. From Figures 17 and 18 it can be seen how the contribution of supercapacitors in the take off phase ensures that there is a considerable saving in the state of charge of the batteries, thus favoring a lightening of weight, an increase in Cycle Life and a safety improvement. Finally, the current generated by the battery pack is analyzed in Figure 19. Having established that the current never approaches the charge or discharge limits, there is no risk of overcurrent, an indispensable prerequisite to avoid damaging the batteries [52]. After these evaluations it is possible to state that all the constraints imposed in the optimization phase have been respected. From the selected solution, an overall emissions balance of $4965kgCO_2$ is obtained, of which $4940kgCO_2$ produced by the

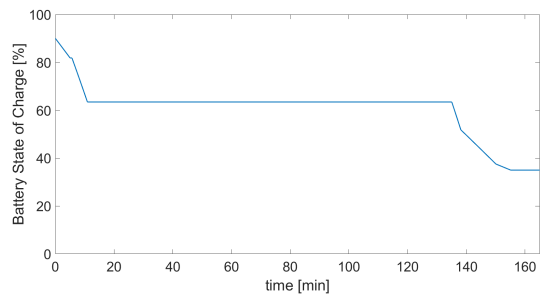


Figure 17: Trend of the battery pack state of charge during the mission.

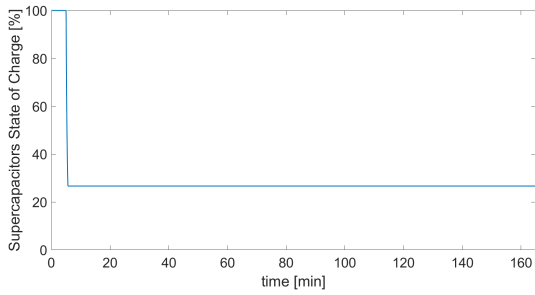


Figure 18: Trend of the supercapacitors state of charge during the mission.

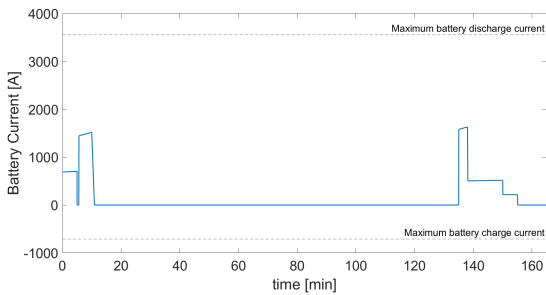


Figure 19: Trend of the current outgoing from the battery pack during the course of the mission.

fuel combustion, $20kgCO_2$ caused by recharging the electric energy accumulators and $5kgCO_2$ generated during the production of batteries, the comparison between these results is shown in Figure 20. Having determined that the plane has 50 passengers in a distance of 1240 km, it follows that $80gCO_2/km$ are issued for each passenger. Assuming that the battery is recharged using renewable energy sources, and thus eliminating the environmental impact due to the recharging of the electrical part, we obtain that the L.E.A.F. aircraft emits $79gCO_2/km$ per passenger. Comparing this data with the reference aircraft it follows that, according to official data [53], the ATR 42 emits $93gCO_2$ per passenger per kilometer, while the ATR 72 emits $69gCO_2$ [54]. However, it is necessary to consider that the data reported refer to Tank to Wing (TtW) analysis which only count the emissions generated in the flight phase, omitting the contri-

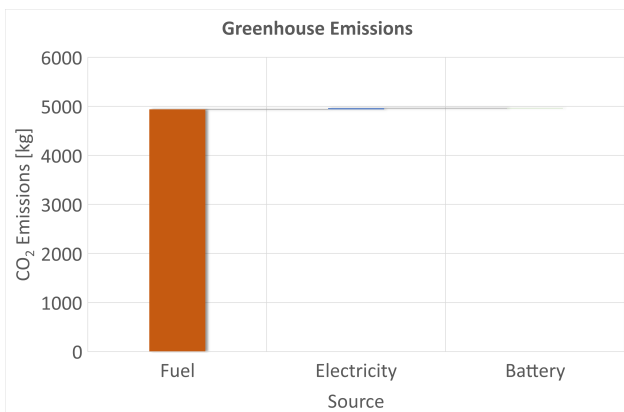


Figure 20: Analysis of CO_2 emissions based on the source considered.

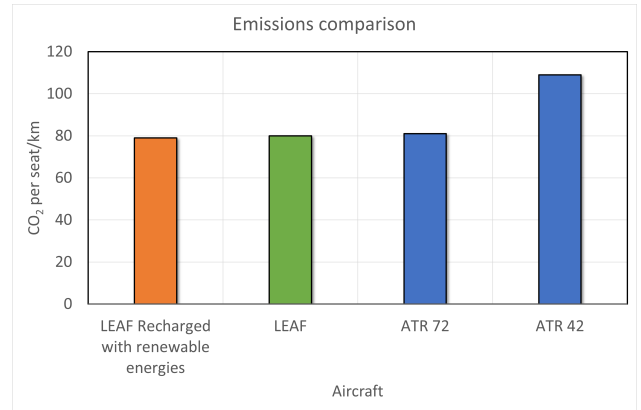


Figure 21: Comparison in terms of emissions between the proposed aircraft and the reference aircraft.

425 bution due to the transport of the fuel to the refueling stations or the recharging of the electric accumulators, nor the production of the battery pack. Applying the reasoning seen in Paragraph 2.7.1 in such a way as to consider the share of emissions due to the transport of the fuel to the refueling station, it happens that the ATR 72 and ATR 42 aircraft emit 81 and $109gCO_2$ per passenger / kilometer respectively. Figure 21 shows a comparison between the emissions of the aforementioned aircraft. The L.E.A.F. project is distinguished by the extent of emissions similar to that referred to the ATR 72, a non-trivial result since the latter has a significantly higher number of passengers (74), therefore with reduced normalized emissions. Compared with the ATR 42, a saving of 27% in emissions is determined for each passenger for each kilometer. It is observed that the recharging of the battery carried out using a renewable energy source entails a further advantage which in the long term assumes an important role.

With this project, the significant potential deriving from the hybridization of aircraft has been ascertained. However, it should be noted that some of the data used are not certain, while others refer to expected values for the future, sometimes with excessively hopeful criteria. Indeed:

- Electric accumulators can be charged by different sources which generate a different amount of emissions [55].
- Kelly et al. [43] claim that, under the most unfavorable conditions, battery production causes emissions of $140kgCO_2/kWh_{batt}$.
- In the analysis, reference was made to the Cycle Life of the batteries but they can undergo degradation phenomena independent of their use which lead to the determination of a Calendar Life [56], from this it follows that, to make the most of the useful life of the battery pack, it must be used continuously.

Therefore, Table 8 shows a sensitivity analysis of the data listed on CO_2 emissions.

Table 8: Sensitivity analysis of some data used.

Parameter	Sensitivity
Electric Energy Source	0.42%
Battery Pack Production	0.10%
Battery Cycle Life	0.09%

460 Among the parameters listed, the one that has the greatest influence is the energy source used to power the storage systems, it follows that, for powertrain systems, in order to create increasingly efficient and low environmental impact aircraft, research and development of increasingly available and low-emission energy sources are important.

465

3.2. Cost analysis

The estimation of the cost of developing an aircraft is an essential part of any aircraft's design process. During conceptual design, the design can still be changed easily, and different approaches to a set of top-level requirements can be tried and evaluated. When hybrid-electric propulsion systems are assessed, costs are a significant consideration. As the propulsion system comprises a large part of total aircraft cost, the addition of an electric power system cannot be neglected. It is chosen to modify existing cost models to include correction factors for hybrid-electric general aviation. To estimate the development and procurement cost of a new aircraft, Eastlake's GA DAPCA-IV model is modified [57]. It requires extra adjustment factors that consider the additional effort that the implementation of a hybrid-electric propulsion system requires. When estimating the operating costs, predominantly Variable Direct Operating Costs (VDOC) components need to be adjusted for hybrid-electric aircraft. Energy and battery cost represent additional components as part of VDOC, and the calculation of maintenance costs differs. In this sense, König et al. [58] state that in 2030 batteries will have a production cost per unit of energy of 150 €/kWh while according to Child et al. [59] in the year 2040 electricity will cost 0.055 €/kWh. Regarding the price of fuel, for the future the literature mainly refers to e-fuels, these are obtained from the combination of hydrogen and CO₂ absorbed from the atmosphere [60], this solution has a significant advantage, given that the amount of carbon dioxide emitted is equal to that recovered from the atmosphere; however, to effectively have a neutral emissions balance, the reforming process that leads to the production of hydrogen must be powered by renewable energy sources. In particular, Zhou et al. [61] estimate that in the year 2040, e-kerosene will cost 8\$/Gallon in Europe. Additionally, as the sales price of hybrid-electric aircraft changes, the fixed operating cost change as well. DAPCA-IV model establishes Cost estimation relationships (CERs) that predict acquisition cost based on design parameters like mass and speed [8]. Eastlake and Blackwell [57] adapted and modified the original DAPCA-IV model, by adjusting the CERs according to the specific differences in the effort required to design general aviation aircraft. CERs for hybrid-electric aircraft have increased. The total engineering effort is expected to be 1/3 higher than

CER Category	F _{Cert} Factor for certification	F _{Comp} Factor for 100% composites	F _{Taper} Factor for untapered wings	F _{CF} Factor for complex flap system	F _{Press} Factor for pressurized cabin	F _{HE} Factor for hybrid-electric propulsion
Engineering Cost	0.67	2.00	-	1.03	1.03	1.33-1.66
Tooling Cost	-	2.00	0.95	1.02	1.01	1.10
Manufacturing Cost	0.75	1.25	-	1.01	-	1.10
Development Support Cost	0.50	1.50	-	1.01	1.03	1.05
Flight Test Operations Cost	0.50	-	-	-	-	1.50
Quality Control Cost	0.50	1.50	-	-	-	1.50
Materials Cost	0.75	-	-	1.02	1.01	1.05

Figure 22: Correction factors to establish CERs

a comparable aircraft with a hybrid-electric propulsion system. The cost of tooling is expected to increase approximately 10 %, as additional fixtures must be put in place to hold the new systems. Analog to the cost for tooling, a 10 % increase in manufacturing cost is expected. The increasing complexity of assembling the propulsion system and all sub-systems will increase the required manufacturing time. The overhead cost is expected to increase slightly (approximately 5 %), as a larger, and more specifically trained workforce will be used to deliver a certified aircraft. The additional complexity of the propulsion system will require a large increase in flight test hours. The authors believe that a 50 % increase in flight test time, and consequently flight test cost, is reasonable. Similarly to the increased flight test cost, the cost of quality control will increase significantly. Again, a 50 % increase is expected. The cost to fabricate hybrid-electric aircraft will only be slightly increased (about a 5% increase is expected). The value of the correction factors are shown in Figure 22. While it could be argued that the degree of hybridization of power HP will influence cost, this is most likely not a strong driver of the total cost. While the individual cost of Internal Combustion Engines (ICE), Electric Motors (EM), and battery will be driven by the degree of hybridization, the engineering and integration effort will remain almost constant, regardless of the power split.

$$H_p = \frac{P_{EM}}{P_{EM} + P_{ICE}} \quad (24)$$

The variable costs include the addition of the cost of electricity for recharging the batteries. A recent study of automotive charging stations revealed that charging efficiency η_{charge} ranges between 82 % and 92 % [62]. A value of $\eta_{charge}=0.85$ is recommended. The maintenance cost of hybrid-electric aircraft is not adjusted, compared to aircraft with conventional propulsion systems. While EMs require less maintenance than ICEs, it is assumed that the additional complexity of a hybrid-electric system and will outweigh this benefit. This assessment is backed by [63], who analyzed maintenance cost for hybrid-electric vehicles and found little difference between the total maintenance cost of a conventional car and a hybrid-electric car. Only by moving towards a fully electric propulsion architecture maintenance cost are reduced by 9 %. It is unlikely that the same amount of savings can be realized for aerospace applications. Therefore, this reduction is neglected in this model. Among

Table 9: Cost analysis for single aircraft.

Feature	Cost per Unit
Engineering	1.856066 US\$
Tooling	298.113 US\$
Manufacturing	1.590.000 US\$
Development Support	50.106 US\$
Flight test operations	27.536 US\$
Quality control	69.760 US\$
Materials	347.620 US\$
Combustion Engine	1.840.000 US\$
Electric motor	40.000 US\$
Power management system	34.000 US\$
Battery	75.195 US\$
Misc	16.500 US\$
COST TO PRODUCE	6.244.896 US\$
Insurance	923.160 US\$
Profit (10% of Cost to Produce)	435.720 US\$
QFD (Quantity Discount Factor)	69%

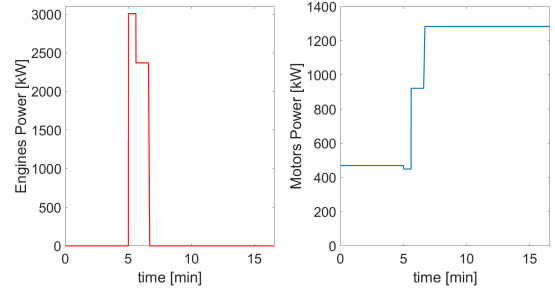


Figure 23: Comparison between the power supplied by the turboprop and that supplied by the electric motors during the safe landing mission.

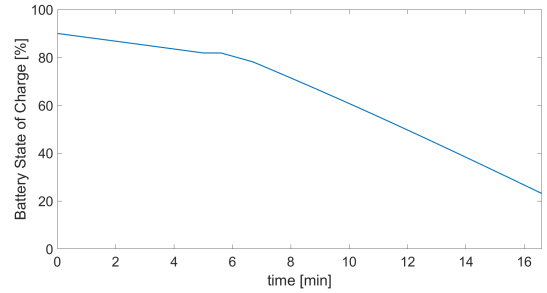


Figure 24: Battery state of charge trend during the safe landing mission.

Fixed Direct Operating Costs (FDOC) include the Battery Depreciation C_{BATD} . It is reasonable to assume that the aircraft's battery will reach its end-of-life state much earlier than the airframe. Kreimeier [64] recommends to depreciate the battery linearly and assumes a life of 1000 full charge and discharge cycles (n_{cycles}). The DAPCA-IV cost estimation method for GA aircraft is modified to capture the effects of implementing advanced propulsion systems on the development and procurement cost. The selection of a hybrid-electric propulsion system will increase aircraft procurement cost by about 17 % to 20 % . However, this figure is expected to be lower for future aircraft that take advantage of the rapid progression of technology development in the field of electric propulsion. Methods that capture the change in operating costs are considered as well, and especially the variable direct operating cost components are supplemented or adjusted. Ultimately, a detailed analysis of the costs necessary for the production of the aircraft is shown in Table 9.

3.3. Safety analysis

To assess the safety of the aircraft, 60 s after the take off phase, therefore when the aircraft is in the climb phase, a failure of the engines was assumed. Consequently, a safe landing was put in place using only electric motors, this test was proposed by Donateo and Cavalera [65]. From the circumstance described, a comparison was derived, shown in Figure 23, between the power supplied by the turboprop and the power supplied by the electric motors during the mission. As can be seen, following the failure, during the execution of the climb phase the power required by the vehicle is exclusively supplied by the electric motors while in the landing phase a total power of 1283.07kW is required. As described in chapter 2.6.2, the aircraft has four electric motors, each of which is characterized

by a nominal power of 475 kW, it follows that they are sufficient to guarantee the power necessary to carry out the landing phase. It remains to be verified that the energy requirement is also met. Figure 24 represents the state of charge of the battery pack in the continuation of the described mission. It may be found that the battery has a final state of charge equal to 23%, so it is not completely discharged, therefore it can be assumed that the aircraft, following a failure of both heat engines, is able to perform a landing in safe conditions supplied exclusively by electric propulsion.

Turboprop failure is not the only aspect to consider in terms of safety; in fact, although in the event of a failure of the electric motors it is still possible to perform a safe landing by means of an exclusively thermal propulsion since turboprop are characterized by a much higher power than electric motors, the batteries used to power the latter are subject to significant risks such as electrical risk, fire risk and the emission of toxic substances [66]. These risks must be mitigated through appropriate prevention and protection strategies, Roshan [67] has proposed a flooding system based on N_2 and O_2 for fire risk protection which is activated by means of a signal sent by a smoke sensor. Furthermore, Hu et al. [68] through an Fault Tree Analysis (FTA) have shown that, in general, the main factors that lead to the fire of an electric vehicle are the materials with low thermal stability and the Battery Management System (BMS) not warned in time. Hence, Guo and Feng [69] have made a Passive Thermal Management (PTM) material capable of satisfying the required conditions in terms of thermal stability while Hashemi et al. [70] proposed an adaptive battery model validated by experimental results to increase the accuracy of their BMS functions such as fault detection. In this adaptive model,

parameters are updated in real time using a supervised machine learning algorithm. Finally, on the basis of tested samples, Du et al. [71] determined that charging rates above 3 C can significantly affect the life and safety performance of the batteries, given that a value equal to 1 C was defined as the charge limit for the batteries considered, by means of an appropriate BMS management it is possible to ensure that this value is not exceeded.

4. Conclusions

The increasingly significant scarcity of raw materials, the consequences of global warming and the energy crisis are pushing towards new frontiers that increasingly aim at electrification and energy efficiency in the transport sector. In this work an alternative solution to an already existing conventional aircraft has been proposed through the aid of technologies whose development is expected by the year 2040, the architecture used consists of a parallel hybrid configuration consisting of an array of two turboprop and four electric motors, the latter are powered by batteries possibly assisted by multifunctional supercapacitors. Although it has been observed that fuel savings are severely limited by the low energy density characterizing the batteries, using multi-objective optimization it has been possible to obtain a lowering of normalized CO_2 emissions with respect to the number of passengers and the distance up to 27% compared to the original aircraft. From the analysis, however, it emerged that the type of primary source used for recharging the storage systems has a conspicuous impact on the final emissions balance, from this it can be inferred that for the mitigation of the environmental impact the electrification of the aircraft itself is not sufficient unless accompanied by changes to the energy park that is used. It was also observed that the hybridization carried out brings a considerable advantage in terms of safety in the event of a turboprop failure also by virtue of the fact that the supercapacitors used allow a saving in the state of charge of the battery pack which can be used for the execution of a safe landing, on the other hand, the batteries involve additional risks especially as regards the fire risk, therefore further measures were necessary for the prevention and protection from any damage. To estimate the take-off weight was used a SFC in the worst case (close to max power) because in the bibliography there were not a very large informations, so the fuel mass is over-sized for the flight even because the thermal propulsion is over-sized. To evaluate the emission of carbon dioxide a more accurate study was done, in fact to estimate the flow of fuel mass the SFC was related to the the power required by the engine for each phase of flight. The choice of the over-sized thermal propulsion (in terms of HP) is given by fact that the turboprop in the bibliography are more efficient in terms of SFC than the other turboprop under-sizing. In the future it is possible to develop turboprop with less HP, so less heavy and more efficient in terms of SFC. The electric propulsion cover the L.E.A.F. aircraft have approximately one thousand of kW, to satisfy the requirements of flight, it would be enough two thousand of kW from the thermal power.



Low Emission Aircraft of the Future

References

- [1] T. Yusaf, L. Fernandes, A. R. A. Talib, Y. S. Altarazi, W. Alrefae, K. Kadigama, D. Ramasamy, A. Jayasuriya, G. Brown, R. Mamat, H. A. Dhahad, F. Benedict, M. Laimon, Sustainable aviation—hydrogen is the future, *Sustainability (Switzerland)* 14 (1 2022). doi:10.3390/su14010548.
- [2] C. Friedrich, P. A. Robertson, Hybrid-electric propulsion for automotive and aviation applications, *CEAS Aeronautical Journal* 6 (2015) 279–290. doi:10.1007/s13272-014-0144-x.
- [3] J. Köhler, P. Jeschke, Conceptual design and comparison of hybrid electric propulsion systems for small aircraft, *CEAS Aeronautical Journal* 12 (2021) 907–922. doi:10.1007/s13272-021-00536-4.
- [4] D. Szirczak, I. Jankovics, I. Gal, D. Rohacs, Conceptual design of small aircraft with hybrid-electric propulsion systems, *Energy* 204 (8 2020). doi:10.1016/j.energy.2020.117937.
- [5] J. Ribeiro, F. Afonso, I. Ribeiro, B. Ferreira, H. Policarpo, P. Peças, F. Lau, Environmental assessment of hybrid-electric propulsion in conceptual aircraft design, *Journal of Cleaner Production* 247 (2 2020). doi:10.1016/j.jclepro.2019.119477.
- [6] L. Tom, M. Khowja, G. Vakil, C. Gerada, Commercial aircraft electrification—current state and future scope, *Energies* 14 (12 2021). doi:10.3390/en14248381.
- [7] F. Centracchio, M. Rossetti, U. Iemma, Approach to the weight estimation in the conceptual design of hybrid-electric-powered unconventional regional aircraft, *Journal of Advanced Transportation* 2018 (2018). doi:10.1155/2018/6320197.
- [8] D. Raymer, *Aircraft Design: A Conceptual Approach*, American Institute of Aeronautics and Astronautics, 2018.
- [9] https://www.archweb.it/dwg/aerei_elicotteri/aerei_2D/aerei_2D.htm#google_vignette, accessed: 2022-08-03.
- [10] J. Hoelzen, Y. Liu, B. Bensmann, C. Winnefeld, A. Elham, J. Friedrichs, R. Hanke-Rauschenbach, Conceptual design of operation strategies for hybrid electric aircraft, *Energies* 11 (2018) 217. doi:10.3390/en11010217. URL <http://www.mdpi.com/1996-1073/11/1/217>
- [11] D. Mande, J. P. Trovão, M. C. Ta, Comprehensive review on main topologies of impedance source inverter used in electric vehicle applications, *World Electric Vehicle Journal* 11 (6 2020). doi:10.3390/WEVJ11020037.
- [12] J. Zhu, H. Kim, H. Chen, R. Erickson, D. Maksimovic, High efficiency sic traction inverter for electric vehicle applications, *Conference Proceedings - IEEE Applied Power Electronics Conference and Exposition - APEC 2018-March (2018)* 1428–1433. doi:10.1109/APEC.2018.8341204.
- [13] M. A. Rahman, X. Wang, C. Wen, A review of high energy density lithium-air battery technology, *Journal of Applied Electrochemistry* 44 (2014) 5–22. doi:10.1007/s10800-013-0620-8.
- [14] X. Han, L. Lu, Y. Zheng, X. Feng, Z. Li, J. Li, M. Ouyang, A review on the key issues of the lithium ion battery degradation among the whole life cycle, *eTransportation* 1 (8 2019). doi:10.1016/j.etrans.2019.100005.
- [15] R. Cingolani, *Il mondo è piccolo come un'arancia: una discussione semplice sulle nanotecnologie*, Il Saggiatore, 2014.
- [16] R. Reece, C. Lekakou, P. A. Smith, A high-performance structural supercapacitor, *ACS Applied Materials and Interfaces* 12 (2020) 25683–25692. doi:10.1021/acsmi.9b23427.
- [17] R. Glasscock, M. Galea, W. Williams, T. Glesk, Hybrid electric aircraft propulsion case study for skydiving mission, *Aerospace* 4 (9 2017). doi:10.3390/aerospace4030045.

- [18] S. Farokhi, Aircraft propulsion, John Wiley & Sons, 2014.
- [19] T. Donato, A. Carlà, G. Avanzini, Fuel consumption of rotorcrafts and potentiality for hybrid electric power systems, *Energy Conversion and Management* 164 (2018) 429–442. doi:10.1016/j.enconman.2018.03.016. 735
- [20] Tabella valori aria standard, http://www.ibneditore.it/wp-content/uploads/_mat_online/scienze_nav_verde/Tabella%20Valori%20Aria%20Standard.pdf, accessed: 2022-08-03. 735
- [21] Civil turboshaft/turboprop specifications, <https://www.jet-engine.net/civtsspec.htm>, accessed: 2022-08-03. 740
- [22] P. Fletcher, P. P. Walsh, Gas turbine performance, John Wiley & Sons, 2008.
- [23] R. C. Bolam, Y. Vagapov, A. Anuchin, A review of electrical motor topologies for aircraft propulsion. 745
- [24] https://www.automobile-catalog.com/curve/2021/3006515/audi_rs_e-tron_gt.html, accessed: 2022-08-03. 745
- [25] T. Zhao, Propulsive battery packs sizing for aviation applications (2018). URL <https://commons.erau.edu/edt/393>
- [26] V. Viswanathan, A. H. Epstein, Y. M. Chiang, E. Takeuchi, M. Bradley, J. Langford, M. Winter, The challenges and opportunities of battery-powered flight, *Nature* 601 (2022) 519–525. doi:10.1038/s41586-021-04139-1. 750
- [27] A. Misra, Energy storage for electrified aircraft: The need for better batteries, fuel cells, and supercapacitors, *IEEE Electrification Magazine* 6 (2018) 54–61. doi:10.1109/MELE.2018.2849922. 755
- [28] B. Tiede, C. O'Meara, R. Jansen, Battery key performance projections based on historical trends and chemistries, *IEEE*, 2022, pp. 754–759. doi:10.1109/ITEC53557.2022.9814008. URL <https://ieeexplore.ieee.org/document/9814008/> 760
- [29] T. Donato, A. Ficarella, A modeling approach for the effect of battery aging on the performance of a hybrid electric rotorcraft for urban air-mobility, *Aerospace* 7 (5 2020). doi:10.3390/AEROSPACE7050056. 760
- [30] L. Guzzella, A. Sciarretta, Vehicle propulsion systems, Springer-Verlag Berlin Heidelberg, 2013. 765
- [31] R. Xiao, Y. Hu, X. Jia, G. Chen, A novel estimation of state of charge for the lithium-ion battery in electric vehicle without open circuit voltage experiment, *Energy* 243 (3 2022). doi:10.1016/j.energy.2021.123072. 765
- [32] D. Belov, M. H. Yang, Failure mechanism of li-ion battery at overcharge conditions, *Journal of Solid State Electrochemistry* 12 (2008) 885–894. doi:10.1007/s10008-007-0449-3. 770
- [33] M. E. Şahin, F. Blaabjerg, A. Sangwongwanich, A comprehensive review on supercapacitor applications and developments, *Energies* 15 (2 2022). doi:10.3390/en15030674. 775
- [34] H. T. Das, E. B. T. S. Dutta, N. Das, P. Das, A. Mondal, M. Imran, Recent trend of ceo2-based nanocomposites electrode in supercapacitor: A review on energy storage applications, *Journal of Energy Storage* 50 (6 2022). doi:10.1016/j.est.2022.104643. 775
- [35] J. Kowal, E. Avaroglu, F. Chamekh, A. Şenfelds, T. Thien, D. Wijaya, D. U. Sauer, Detailed analysis of the self-discharge of supercapacitors, *Journal of Power Sources* 196 (2011) 573–579. doi:10.1016/j.jpowsour.2009.12.028. 780
- [36] C. K. Cheung, S. C. Tan, C. K. Tse, A. Ioinovici, On energy efficiency of switched-capacitor converters, *IEEE Transactions on Power Electronics* 28 (2013) 862–876. doi:10.1109/TPEL.2012.2204903. 785
- [37] L. Guzzella, A. Amstutz, Cae tools for quasi-static modeling and optimization of hybrid powertrains, *IEEE Transactions on Vehicular Technology* 48 (1999) 1762–1769. doi:10.1109/25.806768. 785
- [38] A. Javaid, O. Khalid, A. Shakeel, S. Noreen, Multifunctional structural supercapacitors based on polyaniline deposited carbon fiber reinforced epoxy composites, *Journal of Energy Storage* 33 (1 2021). doi:10.1016/j.est.2020.102168. 790
- [39] P. Jochem, S. Babrowski, W. Fichtner, Assessing co2 emissions of electric vehicles in germany in 2030, *Transportation Research Part A: Policy and Practice* 78 (2015) 68–83. doi:10.1016/j.tra.2015.05.007. 795
- [40] H. Ma, F. Balthasar, N. Tait, X. Riera-Palou, A. Harrison, A new comparison between the life cycle greenhouse gas emissions of battery electric vehicles and internal combustion vehicles, *Energy Policy* 44 (2012) 160–173. doi:10.1016/j.enpol.2012.01.034. 800
- [41] https://ghgprotocol.org/sites/default/files/Emission_Factors_from_Cross_Sector_Tools_March_2017.xlsx, accessed: 2022-08-06. 800
- [42] T. Donato, A. Ficarella, A methodology for the comparative analysis of hybrid electric and all-electric power systems for urban air mobility, *Energies* 15 (1 2022). doi:10.3390/en15020638. 800
- [43] J. C. Kelly, Q. Dai, M. Wang, Globally regional life cycle analysis of automotive lithium-ion nickel manganese cobalt batteries, *Mitigation and Adaptation Strategies for Global Change* (2019). doi:10.1007/s11027-019-09869-2. 800
- [44] N. I. Shchurov, S. I. Dedov, B. V. Malozhomov, A. A. Shtang, N. V. Martyushev, R. V. Klyuev, S. N. Andriashin, Degradation of lithium-ion batteries in an electric transport complex, *Energies* 14 (12 2021). doi:10.3390/en14238072. 800
- [45] D. L. Thompson, J. M. Hartley, S. M. Lambert, M. Shiref, G. D. Harper, E. Kendrick, P. Anderson, K. S. Ryder, L. Gaines, A. P. Abbott, The importance of design in lithium ion battery recycling—a critical review, *Green Chemistry* 22 (2020) 7585–7603. doi:10.1039/d0gc02745f. 800
- [46] F. Re, Viability and state of the art of environmentally friendly aircraft taxiing systems, *Electrical Systems for Aircraft, Railway and Ship Propulsion, ESARS* (2012). doi:10.1109/ESARS.2012.6387462. 800
- [47] A. E. Scholz, D. Trifonov, M. Hornung, Environmental life cycle assessment and operating cost analysis of a conceptual battery hybrid-electric transport aircraft, *CEAS Aeronautical Journal* 13 (2022) 215–235. doi:10.1007/s13272-021-00556-0. 800
- [48] R. Aguilar-Rivera, M. Valenzuela-Rendón, J. Rodríguez-Ortiz, Genetic algorithms and darwinian approaches in financial applications: A survey, *Expert Systems with Applications* 42 (2015) 7684–7697. doi:10.1016/j.eswa.2015.06.001. URL <https://linkinghub.elsevier.com/retrieve/pii/S0957417415003954> 800
- [49] Y. Yusoff, M. S. Ngadiman, A. M. Zain, Overview of nsga-ii for optimizing machining process parameters, *Procedia Engineering* 15 (2011) 3978–3983. doi:10.1016/j.proeng.2011.08.745. 800
- [50] F. Nicolosi, S. Corcione, V. Trifari, A. D. Marco, Design and optimization of a large turboprop aircraft, *Aerospace* 8 (5 2021). doi:10.3390/aerospace8050132. 800
- [51] R. O. Ottosson, P. E. Engström, D. Sjöström, C. F. Behrens, A. Karlsson, T. Knöös, C. Ceberg, The feasibility of using pareto fronts for comparison of treatment planning systems and delivery techniques, *Acta Oncologica* 48 (2009) 233–237. doi:10.1080/02841860802251559. 800
- [52] M. G. Gebremichael, Overcurrent protection circuit for engine starting mode of range extended electric vehicles, *Arabian Journal for Science and Engineering* (2022). doi:10.1007/s13369-022-06807-4. 800
- [53] Atr42-600 the ideal local commuter, https://www.atr-aircraft.com/wp-content/uploads/2022/06/ATR_Fiche42-600-3.pdf, accessed: 2022-08-13. 800
- [54] Atr72-600 the first choice for operators, https://www.atr-aircraft.com/wp-content/uploads/2022/06/ATR_Fiche72-600-3.pdf, accessed: 2022-08-13. 800
- [55] A. R. Holdway, A. R. Williams, O. R. Inderwildi, D. A. King, Indirect emissions from electric vehicles: Emissions from electricity generation, *Energy and Environmental Science* 3 (2010) 1825–1832. doi:10.1039/c0ee00031k. 800
- [56] R. L. Fares, M. E. Webber, What are the tradeoffs between battery energy storage cycle life and calendar life in the energy arbitrage application?, *Journal of Energy Storage* 16 (2018) 37–45. doi:10.1016/j.est.2018.01.002. 800
- [57] C. N. Eastlake, H. W. Blackwell, Cost estimating software for general aviation aircraft design (2000). 800
- [58] A. König, L. Nicoletti, D. Schröder, S. Wolff, A. Waclaw, M. Lienkamp, An overview of parameter and cost for battery electric vehicles, *World Electric Vehicle Journal* 12 (2021) 1–29. doi:10.3390/wevj12010021. 800
- [59] M. Child, C. Kempfert, D. Bogdanov, C. Breyer, Flexible electricity generation, grid exchange and storage for the transition to a 100system in europe, *Renewable Energy* 139 (2019) 80–101. doi:10.1016/j.renene.2019.02.077. 800
- [60] H. Ababneh, B. H. Hameed, Electrofuels as emerging new green alternative fuel: A review of recent literature, *Energy Conversion and Management* 254 (2 2022). doi:10.1016/j.enconman.2022.115213. 800
- [61] Y. Zhou, S. Searle, N. Pavlenko, Current and future cost of e-kerosene in the united states and europe (2022). 800

URL www.theicct.org

- 805 [62] Elektroautos im test: So hoch ist der stromverbrauch, <https://www.adac.de/rund-ums-fahrzeug/tests/elektromobilitaet/stromverbrauch-elektroautos-adac-test/?redirectId=quer.Elektroautos%20Ecotest>, accessed: 2022-08-22.
- [63] B. Propfe, M. Redelbach, D. J. Santini, H. Friedrich, Cost analysis of plug-in hybrid electric vehicles including maintenance & repair costs and resale values, *World Electric Journal* (2012).
810 URL http://www.transportation.anl.gov/modeling_
- [64] M. Kreimeier, Evaluation of on-demand air mobility concepts with utilization of electric powered small aircraft (2018).
- [65] T. Donato, D. Cavalera, Increasing safety in ultralight aviation with a wankel-based series/parallel hybrid electric power system, *Machines* 10 (2022) 486. doi:10.3390/machines10060486.
- 815 [66] H. A. Gabbar, A. M. Othman, M. R. Abdussami, Review of battery management systems (bms) development and industrial standards, *Technologies* 9 (2021) 28. doi:10.3390/technologies9020028.
- [67] R. Sebastian, A review of fire mitigation methods for li-ion battery energy storage system, *Process Safety Progress* (2022). doi:10.1002/prs.12365.
820
- [68] G. Hu, P. Huang, Z. Bai, Q. Wang, K. Qi, Comprehensively analysis the failure evolution and safety evaluation of automotive lithium ion battery, *eTransportation* 10 (11 2021). doi:10.1016/j.etrans.2021.100140.
- 825 [69] X. Guo, J. Feng, Facilely prepare passive thermal management materials by foaming phase change materials to achieve long-duration thermal insulation performance, *Composites Part B: Engineering* 245 (2022) 110203. doi:10.1016/j.compositesb.2022.110203.
URL <https://linkinghub.elsevier.com/retrieve/pii/S1359836822005777>
- 830 [70] S. R. Hashemi, A. B. Baghbadorani, R. Esmaceli, A. Mahajan, S. Farhad, Machine learning-based model for lithium-ion batteries in bms of electric/hybrid electric aircraft, *International Journal of Energy Research* 45 (2021) 5747–5765. doi:10.1002/er.6197.
- 835 [71] J. Du, Y. Liu, X. Mo, Y. Li, J. Li, X. Wu, M. Ouyang, Impact of high-power charging on the durability and safety of lithium batteries used in long-range battery electric vehicles, *Applied Energy* 255 (12 2019). doi:10.1016/j.apenergy.2019.113793.